Popular Summary:

"Modulation of Atlantic Aerosols by the Madden-Julian Oscillation"

Tian, B., D.E. Waliser, R.A. Kahn, and S. Wong, 2010.

J. Geophys. Res., submitted.

Much like the better-known El Nino–Southern Oscillation, the Madden-Julian Oscillation (MJO) is a global-scale atmospheric phenomenon. The MJO involves periodic, systematic changes in the distribution of clouds and precipitation over the western Pacific and Indian oceans, along with differences in wind intensity over even more extensive areas, including the north and sub-tropical Atlantic Ocean. The lead authors of this paper developed a sophisticated mathematical technique for mapping the spatial and temporal behavior of changes in the atmosphere produced by the MJO. In a previous paper, we applied this technique to search for modulation of airborne particle amount in the eastern hemisphere associated with the "wet" (cloudy) vs. "dry" phases of the MJO. The study used primarily AVHRR, MODIS, and TOMS satellite-retrieved aerosol amount, but concluded that other factors, such as cloud contamination of the satellite signals, probably dominated the observed variations.

The current paper looks at MJO modulation of desert dust transport eastward across the Atlantic from northern Africa, a region much less subject to systematic cloud contamination than the eastern hemisphere areas studied previously. In this case, a distinct aerosol signal appears, showing that dust is transported westward much more effectively during the MJO phase that favors westward-flowing wind, and such transport is suppressed when the MJO reduces these winds. Aside form the significant achievement in identifying such an effect, the result implies that an important component of global dust transport can be predicted based on the phase of the MJO. As a consequence, the impact of airborne dust on storm development in the Atlantic, and on dust deposition downwind of the desert sources, can also be predicted and more accurately modeled.

Modulation of Atlantic Aerosols by the Madden-Julian Oscillation

Baijun Tian[1], Duane E. Waliser[1], Ralph A. Kahn[2], and Sun Wong[1]

[1]*Jet Propulsion Laboratory, California Institute of Technology, Pasadena, CA*

[2]*NASA Goddard Space Flight Center, Greenbelt, MD*

Correspondence to: Baijun Tian (baijun.tian@jpl.nasa.gov)

Abstract

Our previous study found large intra-seasonal variations in satellite-derived aerosol products over tropical Atlantic Ocean associated with the Madden-Julian Oscillation (MJO). This study aims to investigate the physical mechanism of these aerosol anomalies through analyzing aerosol optical thickness (AOT) from the MODIS instrument on Aqua satellite and low-level (850-hPa) horizontal winds from NCEP/NCAR reanalysis. Our analysis indicates that when enhanced MJO convection is located over the equatorial Indian Ocean (western Pacific), persistent low-level westerly (easterly) anomalies over the equatorial Atlantic reduce (enhance) the low-level westward aerosol transport from Africa and induce negative (positive) AOT anomalies over the equatorial Atlantic. These results indicate that the MJO modulates the Atlantic aerosol concentration through its influence on the Atlantic low-level zonal wind anomalies and westward aerosol transport from Africa. This study implies that Atlantic aerosol concentration might have predictable components with lead times of 2-4 weeks given the predictability of the MJO.

1. Introduction

The Madden-Julian Oscillation (MJO) [*Madden and Julian*, 1971; 1972] is the dominant form of the intra-seasonal (30–90 day) variability in the tropical atmosphere and is characterized by slow (~5 m s^{-1}) eastward-propagating, large-scale oscillations in the tropical deep convection and baroclinic winds, especially over the warmest tropical waters in the equatorial Indian Ocean and western Pacific, during boreal winter (November-April), when the Indo-Pacific warm pool is centered near the equator [*Lau and Waliser*, 2005; *Zhang*, 2005]. It has been well documented that the MJO can impact numerous physical weather and climate phenomena over the globe. However, the impact of the MJO on atmospheric composition is only beginning to be realized [e.g., *Li et al.*, 2010; *Tian et al.*, 2007; *Weare*, 2010; *Wong and Dessler*, 2007; *Ziemke and Chandra*, 2003].

Recently, *Tian et al.* [2008] examined the aerosol variability related to the MJO using multiple, global satellite aerosol products including aerosol index (AI) from the Total Ozone Mapping Spectrometer (TOMS) on Nimbus-7 satellite, and aerosol optical thickness (AOT) from the Moderate Resolution Imaging Spectroradiometer (MODIS) on Terra satellite and the Advanced Very High Resolution Radiometer (AVHRR) on NOAA satellites. That analysis indicated large intra-seasonal variations in the aerosol products over the whole Tropics (see Figures 2 and 4 of *Tian et al.* [2008]). {Baijun – I suggest this rewording because the variations were in the aerosol *products*, but likely not in the actual aerosols, in this case.} Over the tropical Indian Ocean and western Pacific where MJO convection is active and the background aerosol level is low, a strong inverse linear relationship between the TOMS AI and rainfall anomalies, but a weaker, less coherent *positive* correlation between the MODIS/AVHRR AOT and rainfall anomalies, were found. Although a number of plausible mechanisms for these relationships exist, the exact causes are still to be determined.

Over the equatorial Atlantic Ocean and Africa where MJO convection is weak but the background aerosol level is high, the spatial and temporal patterns of TOMS AI and MODIS AOT anomalies are similar. When the enhanced MJO convection is located over the equatorial Indian Ocean (western Pacific), the aerosol anomalies over the equatorial Atlantic Ocean and Africa are negative (positive). Since the MJO convection and associated cloud anomalies are rather weak over the equatorial Atlantic Ocean and Africa, the cloud contamination effect for the AOT MJO anomalies should be weak too over this region [*Tian et al.*, 2008]. However, how the MJO generates these aerosol variations over the equatorial Atlantic Ocean and Africa was not addressed in *Tian et al.* [2008]. The purpose of the present study is to investigate how the MJO generates these intra-seasonal aerosol variations over the equatorial Atlantic Ocean and modulates the Atlantic aerosol concentration.

Given the potential predictability of the MJO extending to 2-4 weeks [e.g., *Waliser*, 2005], if the MJO does influence the Atlantic aerosols, then the Atlantic aerosol concentration may be predictable with lead times of 2-4 weeks, which in turn may lend important guidance to prediction of air quality, dust storm activity, and ocean nutrient deposition over the Atlantic Ocean. Furthermore, the modulation of Atlantic aerosol by the MJO will provide an important physical/chemical process to evaluate chemical transport models and help model development. Section 2 describes the data sets and analysis methodology used in this study. Section 3 presents the main results followed by conclusions and discussion in Section 4.

2. Data and methodology

For this study, we use the MODIS/Aqua Collection 5.1 (C051), Level-3 (L3) daily global aerosol product 'Optical_Depth_Land_And_Ocean' (MYD08_D3). The data are on $1^\circ \times 1^\circ$ spatial grids and from 4 July 2002 to 1 June 2009. This aerosol product represents total-column AOT at 0.55 μm over both ocean (best) [*Tanre et al.*, 1997] and land (corrected) except for bright surfaces [*Kaufman et al.*, 1997] based on the 'dark target' algorithm [*Remer et al.*, 2005; 2008]. To characterize the large-scale circulation patterns that transport aerosols, daily horizontal winds from the National Centers for Environmental Prediction/National Center for Atmospheric Research (NCEP/NCAR) reanalysis were used. The wind data have a spatial resolution of $2.5^\circ \times 2.5^\circ$ and are from 2002 to 2009.

For the MJO analysis and composite procedure, we use the multivariate empirical orthogonal function (EOF) method introduced by *Wheeler and Hendon* [2004] and adopted widely by the MJO community [e.g., *Waliser et al.*, 2009]. The comparison of this multivariate EOF method and the extended EOF method used in our previous aerosol study [*Tian et al.*, 2008] has been examined by *Tian et al.* [2010] with the finding that both methods yield similar results for the MJO composite analysis. Briefly, the intra-seasonal anomalies of daily aerosol and wind data were obtained by removing the climatological-mean seasonal cycle and filtering via a 30–90-day band pass filter. Then, a composite MJO cycle (8 phases) was calculated by averaging the daily anomalies that occurred within each phase of the MJO cycle. The MJO phase for each day is determined by the Real-time Multivariate MJO (RMM) index (a pair of PC time series called RMM1 and RMM2; available from 1974 to present at http://www.cawcr.gov.au/bmrc/clfor/cfstaff/matw/maproom/RMM/). Figure 1 shows the (RMM1, RMM2) phase space for all days in boreal winter from November 2002 to April 2009 and the number of days for each phase of the composite MJO cycle. Only days with strong MJO activity ($RMM1^2+RMM2^2>=1$) are considered. The statistical assessment as to whether a composite mean at each point is different from zero is assessed by the two-sided t test, $t = \sqrt{N}\bar{x}/\sigma$. Here, N is the number of samples in the composite mean and in this case the number of days for each phase of the composite MJO cycle. $\bar{x}$ and σ are the composite mean and standard deviations of the AOT samples for each phase of the composite MJO cycle.

3. Results

Figure 2a shows the climatological mean (2002-2009) boreal winter MODIS/Aqua AOT and NCEP/NCAR 850-hPa horizontal winds over the tropical Atlantic and nearby region (90°W-50°E, 40°S-40°N). In Figure 2a, the strong impact of land surface emission and large-scale horizontal, especially zonal, wind transport are evident in the aerosol distribution. For example, large aerosol loadings are found near the Sahara and Arabian deserts due to strong sources of desert dust and over equatorial Africa and Amazon associated with biomass burning activities [*Kaufman et al.*, 2005]. The dominant aerosol feature over the tropical Atlantic is the zonally oriented optically thick aerosol plume centered at 5°N-8°N stretching across the Atlantic. Its magnitude (>0.6) and latitudinal extent (~15°S - 20°N) are greatest over the eastern equatorial Atlantic along the west coast of Africa and gradually decrease westward toward the central and western equatorial Atlantic. It can reach the northeast coast of South America and Amazon basin with sizable AOT values (~0.2). This aerosol plume is the result of the equatorial Atlantic trade winds that transport the mixed Saharan/Sahelian dust and biomass-burning smoke from Africa to the Atlantic Ocean [e.g., *Cakmur et al.*, 2001; *Carlson and Prospero*, 1972; *Huang et al.*, 2010; *Husar et al.*, 1997; *Kaufman et al.*, 2005]. Over the midlatitude Atlantic (~40°N/S), there is a relatively high aerosol loading (~0.15) that is associated with the midlatitude westerlies that transport the industrial pollution (sulfate and carbonaceous aerosols) from South and North America to the Atlantic Ocean. Over the subtropical North and South Atlantic (~25°N/S), two high-pressure anticyclones (e.g., Azores high) dominate and the aerosol loading there is very low (~0.05).

Figure 2b shows the similar map as Figure 2a except for the 700-hPa NCEP/NCAR horizontal winds. Comparing Figure 2a and 2b indicates that the large-scale circulation patterns are roughly similar between 850 and 700 hPa, such as the equatorial trade winds and subtropical highs. Thus, both wind patterns can explain the gross aerosol distribution pattern. However, there are two notable differences. First, over the Gulf of Guinea, the easterly wind speed is much larger at 700 hPa than at 850 hPa and a correlation analysis indicates that the linear correlation between the mean AOT and westerly wind speed is higher at 700-hPa than at 850 hPa. Thus, the 700-hPa winds may play a more important role in transporting the aerosol over this region. {Includes smoke and some dust.} Second, over the Saharan desert and west coast of Africa near 20°N, northeasterly trade winds dominate at 850 hPa, whereas westerlies are common at 700 hPa. Thus, the aerosol (mostly dust) over the west coast of Africa near 20°N is more likely transported by the 850-hPa winds instead of the 700-hPa winds as first noted by

Chiapello et al. [1995]. Recent work of *Huang et al.* [2010] (their Figure 12h) also shows that the typical dust height is much lower in winter (around 1-2 km) than summer (around 3-4 km). Thus, we choose 850-hPa instead of 700-hPa winds for the analysis results presented here.

Figure 3 shows the composite maps of boreal winter MJO-related MODIS/Aqua AOT anomalies (multiplied by 100 and with 95% confidence limits based on a Student's t-test) and 850-hPa NCEP/NCAR horizontal wind anomalies over the tropical Atlantic region (70°W-30°E, 20°S-30°N). In Figure 3 we see large AOT anomalies over the equatorial Atlantic, collocated with the background aerosol plume (Figure 2). The highest magnitude (±0.04) and largest latitudinal extent (~15°S - 20°N) of these AOT anomalies are typically found over the eastern equatorial Atlantic along the west coast of Africa. The AOT anomalies range up to about ±0.04 for the composite MJO and are about 20% of their background mean (~0.2) (Figure 2). However, the AOT anomalies for individual MJO events are about ±0.2 and can be as large as ±0.8. These AOT anomalies for individual MJO events are much larger than MODIS AOT uncertainty (±0.03) [*Remer et al.*, 2005; 2008] and comparable to the AOT anomalies caused by dust storms at synoptic scale (~0.2) [*Wong et al.*, 2006]. To demonstrate the importance of the intra-seasonal variations of the Atlantic aerosols in their overall variability, Figure 4 shows the standard deviations of boreal winter AOT anomalies after removing the mean seasonal cycle (>= 2 days, total) (4a) and those for the intra-seasonal time scale after removing the mean seasonal cycle and filtering via a 30–90-day band pass filter (note color scale change) (4b) as well as the percentage of the total variance of boreal winter AOT anomalies explained by their intra-seasonal variance (4c). The spatial patterns of the standard deviations of boreal winter AOT anomalies for both total and intra-seasonal time scales are similar to that of the mean AOT in Figure 2. The magnitude of the total standard deviations is about half of that of the means. Furthermore, the magnitude of the intra-seasonal standard deviation is about half of that of the total anomalous (apart from the seasonal cycle) standard deviations. As is evident, the intra-seasonal variance accounts for about 25% of the total variance of the aerosol variability over the tropical Atlantic (e.g., 5°S-15°N). Thus, intra-seasonal variability, and even that part driven by the MJO, is one of the most important forms of Atlantic aerosol variability.

For a comparison between the current MODIS/Aqua results and our earlier MODIS/Terra results, the phases 2, 4, 6, and 8 in the current Figure 3 (hereafter CF3) roughly correspond to the lags 0, +2, +4, and -2 in Figure 4 of *Tian et al.* [2008] (hereafter OF4) according to the location of MJO convection (rainfall) anomalies (see Figure 4 of *Tian et al.* [2008] and Figure 12 of *Waliser et al.* [2009]). Comparing these two figures indicates that the general spatial and temporal patterns and magnitudes of AOT anomalies over the Atlantic region are similar between MODIS/Aqua and MODIS/Terra. For example, both phase 2 in CF3 and lag 0 in OF4 show strong negative AOT anomalies over the tropical Atlantic when the enhanced convection is located over the central and eastern equatorial Indian Ocean. In contrast, both phase 6 in CF3 and lag +4 in OF4 show strong positive AOT anomalies over the tropical Atlantic when the enhanced convection is located over the equatorial western Pacific. Furthermore, both phase 4 in CF3 and lag +2 in OF4 show weak positive AOT anomalies over the tropical North Atlantic and weak negative AOT anomalies over the tropical South Atlantic when the enhanced convection is located over the Maritime Continent, and conversely for phase 8 in CF3 and lag -2 in OF4. The global spatial and temporal patterns of MODIS/Aqua and MODIS/Terra AOT anomalies are also similar (not shown).

Figure 3 also demonstrates the strong impact of low-level horizontal, especially zonal, wind anomalies on the Atlantic AOT anomalies. For example, at phase 2 when the enhanced convection is located over the central and eastern equatorial Indian Ocean (Figure 12 of *Waliser et al.* [2009]), the 850-hPa horizontal wind anomalies over the equatorial Atlantic are persistent westerlies that blow from the Atlantic Ocean to Africa as a dynamical response to the enhanced convection over the Indian Ocean. These westerly anomalies suppress the background westward aerosol transport by the low-level mean easterlies and cause the negative AOT anomalies over the Atlantic region. A similar argument can also be applied to phases 1 and 3. In contrast, in phase 6 when the enhanced MJO convection is located over the equatorial western Pacific (Figure 12 of *Waliser et al.* [2009]), the 850-hPa horizontal wind anomalies over the equatorial Atlantic are persistent easterlies that blow from Africa to the Atlantic Ocean as a dynamical response to suppressed convection over the Indian Ocean. These easterly anomalies enhance the background westward aerosol transport by the low-level mean easterlies and cause the positive AOT anomalies over the Atlantic region. Similar reasoning also applies to phases 4 and 5. To better demonstrate the important role of low-level zonal wind anomalies in the Atlantic AOT anomalies, Figure 5 shows the linear correlation coefficient between the MODIS/Aqua AOT anomalies for the composite MJO cycle (Figure 3) and 850-hPa NCEP/NCAR zonal wind anomalies for the composite MJO cycle over the tropical Atlantic region. Here, negative (positive) correlation means that westerly anomalies induce negative (positive) AOT anomalies or easterly anomalies induce positive (negative) AOT anomalies. Clearly, the AOT anomalies are negatively correlated with the 850-hPa zonal wind anomalies over most part of tropical Atlantic and the west coast of Africa. The largest negative correlation (~ -0.9) is found over the south equatorial Atlantic and western Africa (10°S-EQ, 0°-30°E). These results indicate that the intra-seasonal aerosol variations over the tropical Atlantic are produced by the low-level zonal wind anomalies over the Atlantic associated with the MJO. In other words, the MJO modulates the Atlantic aerosols through its influence on the Atlantic low-level zonal wind anomalies and westward aerosol transport from Africa. It is also interesting to note a positive correlation between AOT and zonal wind over the east coast of South America around (15°S, 40°W) where the background trade winds blow the clean marine air from south Atlantic to South America (Figure 2). Thus, westerly (easterly) anomalies will reduce (enhance) the marine air input to the land and enhance (suppress) the local biomass burning activity and aerosol loading. The 700-hPa winds were also examined and the results are very similar those from 850 hPa.

4. Conclusions and discussion

This study aims to investigate the physical mechanism of large intra-seasonal variations in tropical Atlantic aerosols found in our previous study [*Tian et al.*, 2008] through analyzing the MODIS/Aqua AOT and NCEP/NCAR 850-hPa horizontal winds. First, through reference to our earlier study, we show that the general spatial and temporal patterns and magnitudes of AOT anomalies over the Atlantic region are similar between MODIS/Aqua and MODIS/Terra. The intra-seasonal variance related to the MJO accounts for about 25% of the total variance of MODIS/Aqua AOT over the tropical Atlantic. Thus, the intra-seasonal variability is one of the most important forms of Atlantic aerosol variability. Second, we show that when enhanced MJO convection is located over the equatorial Indian Ocean, persistent low-level westerly anomalies over the equatorial Atlantic suppress the background westward aerosol transport and cause the negative AOT anomalies over the Atlantic region. In contrast, when enhanced MJO convection is located over the equatorial western Pacific, persistent low-level easterly anomalies over the equatorial Atlantic enhance the background westward aerosol transport and cause the positive AOT anomalies over the Atlantic region. These results indicate that the intra-seasonal aerosol variations over the tropical Atlantic are produced by the low-level zonal wind anomalies over the Atlantic associated with the MJO. In other words, the MJO modulates the Atlantic aerosols through its influence on the Atlantic low-level zonal wind anomalies and westward aerosol transport from Africa. Given the potential predictability of the MJO extending to 2-4 weeks [e.g., *Waliser*, 2005], this study implies that components of the Atlantic aerosol concentration may be predictable with lead times of 2-4 weeks, which in turn may lend important guidance to the climate processes, such as air quality, dust storm, and ocean nutrients, over the Atlantic Ocean. Furthermore, this study will provide an important physical/chemical process to evaluate chemical transport models and help the model development.

Acknowledgments

This research was performed at Jet Propulsion Laboratory (JPL), California Institute of Technology, under a contract with NASA. It was supported in part by the Atmospheric Infrared Sounder (AIRS) project at JPL and the National Science Foundation (NSF) grant ATM-0840755 at University of California, Los Angeles.

References

Cakmur, R. V., R. L. Miller, and I. Tegen (2001), A comparison of seasonal and interannual variability of soil dust aerosols over the Atlantic Ocean as inferred by the TOMS AI and AVHRR AOT retrievals, *J. Geophys. Res.*, *106*(D16), 18287-18303.

Carlson, T. N., and J. M. Prospero (1972), The large-scale movement of Saharan air outbreaks over the northern equatorial Atlantic, *J. Appl. Meteorol.*, *11*(2), 283-297, doi:10.1175/1520-0450(1972)011<0283:TLSMOS>2.0.CO;2.

Chiapello, I., G. Bergametti, L. Gomes, B. Chatenet, F. Dulac, J. Pimenta, and E. S. Suares (1995), An additional low layer transport of Sahelian and Saharan dust over the north-eastern tropical Atlantic, *Geophys. Res. Lett.*, *22*(23), 3191-3194.

Huang, J. F., C. D. Zhang, and J. M. Prospero (2010), African dust outbreaks: A satellite perspective of temporal and spatial variability over the tropical Atlantic Ocean, *J. Geophys. Res.*, *115*, D05202, doi:10.1029/2009jd012516.

Husar, R. B., J. M. Prospero, and L. L. Stowe (1997), Characterization of tropospheric aerosols over the oceans with the NOAA Advanced Very High Resolution Radiometer optical thickness operational product, *J. Geophys. Res.*, *102*(D14), 16889-16909.

Kaufman, Y. J., D. Tanre, H. R. Gordon, T. Nakajima, J. Lenoble, R. Frouin, H. Grassl, B. M. Herman, M. D. King, and P. M. Teillet (1997), Passive remote sensing of tropospheric aerosol and atmospheric correction for the aerosol effect, *J. Geophys. Res.*, *102*(D14), 16815-16830.

Kaufman, Y. J., I. Koren, L. A. Remer, D. Tanre, P. Ginoux, and S. Fan (2005), Dust transport and deposition observed from the Terra-Moderate Resolution Imaging Spectroradiometer (MODIS) spacecraft over the Atlantic ocean, *J. Geophys. Res.*, *110*(D10), D10s12, doi:10.1029/2003jd004436.

Lau, W. K. M., and D. E. Waliser (Eds.) (2005), *Intraseasonal Variability of the*

Atmosphere-Ocean Climate System, 474 pp., Springer, Heidelberg, Germany.

Li, K.-F., B. Tian, D. E. Waliser, and Y. L. Yung (2010), Tropical mid-tropospheric CO2 variability driven by the Madden-Julian Oscillation, *Proc. Nat. Acad. Sci.*, in press.

Madden, R. A., and P. R. Julian (1971), Detection of a 40-50 day oscillation in the zonal wind in the tropical Pacific, *J. Atmos. Sci.*, *28*(7), 702-708.

Madden, R. A., and P. R. Julian (1972), Description of global-scale circulation cells in tropics with a 40-50 day period, *J. Atmos. Sci.*, *29*(6), 1109-1123.

Remer, L. A., Y. J. Kaufman, D. Tanre, S. Mattoo, D. A. Chu, J. V. Martins, R. R. Li, C. Ichoku, R. C. Levy, R. G. Kleidman, T. F. Eck, E. Vermote, and B. N. Holben (2005), The MODIS aerosol algorithm, products, and validation, *J. Atmos. Sci.*, *62*(4), 947-973.

Remer, L. A., R. G. Kleidman, R. C. Levy, Y. J. Kaufman, D. Tanre, S. Mattoo, J. V. Martins, C. Ichoku, I. Koren, H. B. Yu, and B. N. Holben (2008), Global aerosol climatology from the MODIS satellite sensors, *J. Geophys. Res.*, *113*(D14), D14s07, doi:10.1029/2007jd009661.

Tanre, D., Y. J. Kaufman, M. Herman, and S. Mattoo (1997), Remote sensing of aerosol properties over oceans using the MODIS/EOS spectral radiances, *J. Geophys. Res.*, *102*(D14), 16971-16988.

Tian, B., Y. L. Yung, D. E. Waliser, T. Tyranowski, L. Kuai, E. J. Fetzer, and F. W. Irion (2007), Intraseasonal variations of the tropical total ozone and their connection to the Madden-Julian Oscillation, *Geophys. Res. Lett.*, *34*(8), L08704, doi:10.1029/2007GL029451.

Tian, B., D. E. Waliser, R. A. Kahn, Q. Li, Y. L. Yung, T. Tyranowski, I. V. Geogdzhayev, M. I. Mishchenko, O. Torres, and A. Smirnov (2008), Does the Madden-Julian Oscillation influence aerosol variability?, *J. Geophys. Res.*, *113*(D12), D12215, doi:10.1029/2007jd009372.

Tian, B., D. E. Waliser, E. J. Fetzer, and Y. L. Yung (2010), Vertical moist thermodynamic structure of the Madden-Julian Oscillation in Atmospheric Infrared Sounder retrievals: An update and a comparison to ECMWF interim reanalysis, *Mon. Wea. Rev.*, *0*(0), doi:10.1175/2010MWR3486.1.

Waliser, D., K. Sperber, H. Hendon, D. Kim, M. Wheeler, K. Weickmann, C. Zhang, L. Donner, J. Gottschalck, W. Higgins, I. S. Kang, D. Legler, M. Moncrieff, F. Vitart, B. Wang, W. Wang, S. Woolnough, E. Maloney, S. Schubert, and W. Stern (2009), MJO simulation diagnostics, *J. Climate*, *22*(11), 3006-3030, 10.1175/2008jcli2731.1.

Waliser, D. E. (2005), Predictability and forecasting, in *Intraseasonal Variability of the Atmosphere-Ocean Climate System*, edited by W. K. M. Lau and D. E. Waliser, pp. 389-424, Springer, Heidelberg, Germany.

Weare, B. C. (2010), Madden-Julian Oscillation in the tropical stratosphere, *J. Geophys. Res.*, *115*, D17113, doi:10.1029/2009jd013748.

Wheeler, M. C., and H. H. Hendon (2004), An all-season real-time multivariate MJO index: Development of an index for monitoring and prediction, *Mon. Wea. Rev.*, *132*(8), 1917-1932.

Wong, S., P. R. Colarco, and A. E. Dessler (2006), Principal component analysis of the evolution of the Saharan air layer and dust transport: Comparisons between a model simulation and MODIS and AIRS retrievals, *J. Geophys. Res.*, *111*(D20), D20109, doi:10.1029/2006jd007093.

Wong, S., and A. E. Dessler (2007), Regulation of H2O and CO in tropical tropopause layer by the Madden-Julian oscillation, *J. Geophys. Res.*, *112*(D14), D14305, doi:10.1029/2006JD007940.

Zhang, C. (2005), The Madden-Julian Oscillation, *Rev. Geophys.*, *43*, RG2003, doi:10.1029/2004RG000158.

Ziemke, J. R., and S. Chandra (2003), A Madden-Julian Oscillation in tropospheric ozone, *Geophys. Res. Lett.*, *30*(23), 2182, doi:10.1029/2003GL018523.

Figure Captions

Figure 1: (RMM1, RMM2) phase space for all days in boreal winter from November 2002 to April 2009 and the number of days for each phase of the MJO cycle. Eight defined phases of the phase space are labeled to indicate the eastward propagation of the MJO in one MJO cycle. Also labeled are the approximate locations of the enhanced convective signal of the MJO for that location of the phase space, e.g., the ''Indian Ocean'' for phases 2 and 3.

Figure 2: (a) Climatological mean (2002-2009) boreal winter (November-April) MODIS/Aqua AOT and NCEP/NCAR 850-hPa horizontal winds over the tropical Atlantic region. White regions indicate areas of missing MODIS/Aqua AOT data. (b) As in (a) except for 700-hPa NCEP/NCAR horizontal winds.

Figure 3: Composite maps of boreal winter (November-April) MJO-related MODIS/Aqua AOT anomalies (multiplied by 100) and NCEP/NCAR 850-hPa horizontal wind (m s^{-1}) anomalies over the tropical Atlantic region. Only AOT anomalies with above 95% confidence limit are shown.

Figure 4: (a) Standard deviation of boreal winter (November-April) MODIS/Aqua AOT anomalies after removing the mean seasonal cycle (>= 2 days, total); (b) Same as (a) except for intraseasonal time scale after removing the mean seasonal cycle and filtering via a 30–90-day band pass filter; (c) Percentage of the total variance of boreal winter MOIDS/Aqua AOT anomalies explained by their intraseasonal variance.

Figure 5: Linear correlation coefficient between boreal winter (November-April) MJO-related MODIS/Aqua AOT anomalies and NCEP/NCAR 850-hPa zonal wind

($m\ s^{-1}$) anomalies over the tropical Atlantic region. Negative (positive) correlation means that westerly anomalies induce negative (positive) AOT anomalies or easterly anomalies induce positive (negative) AOT anomalies.

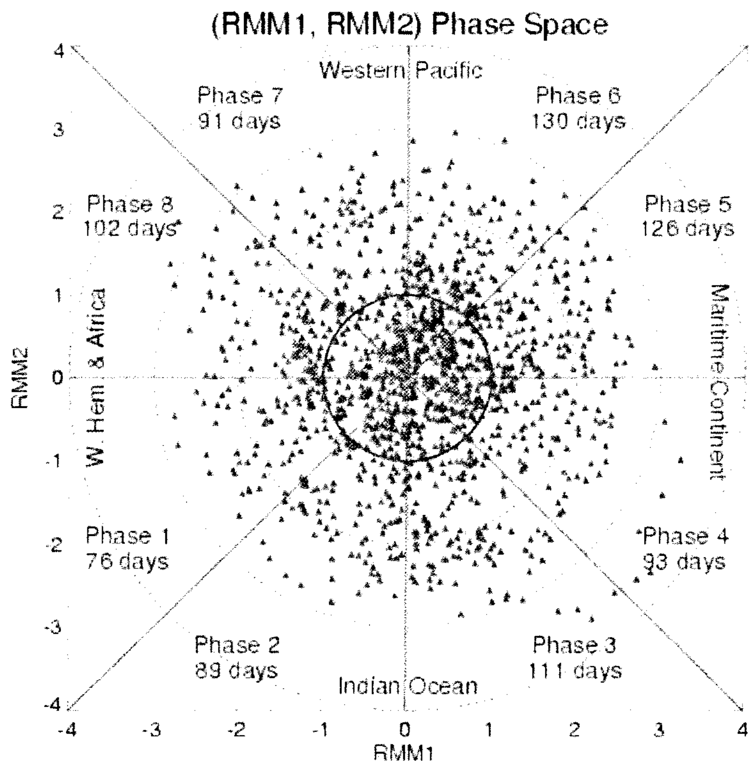

Figure 1: (RMM1, RMM2) phase space for all days in boreal winter from November 2002 to April 2009 and the number of days for each phase of the MJO cycle. Eight defined phases of the phase space are labeled to indicate the eastward propagation of the MJO in one MJO cycle. Also labeled are the approximate locations of the enhanced convective signal of the MJO for that location of the phase space, e.g., the ''Indian Ocean'' for phases 2 and 3.

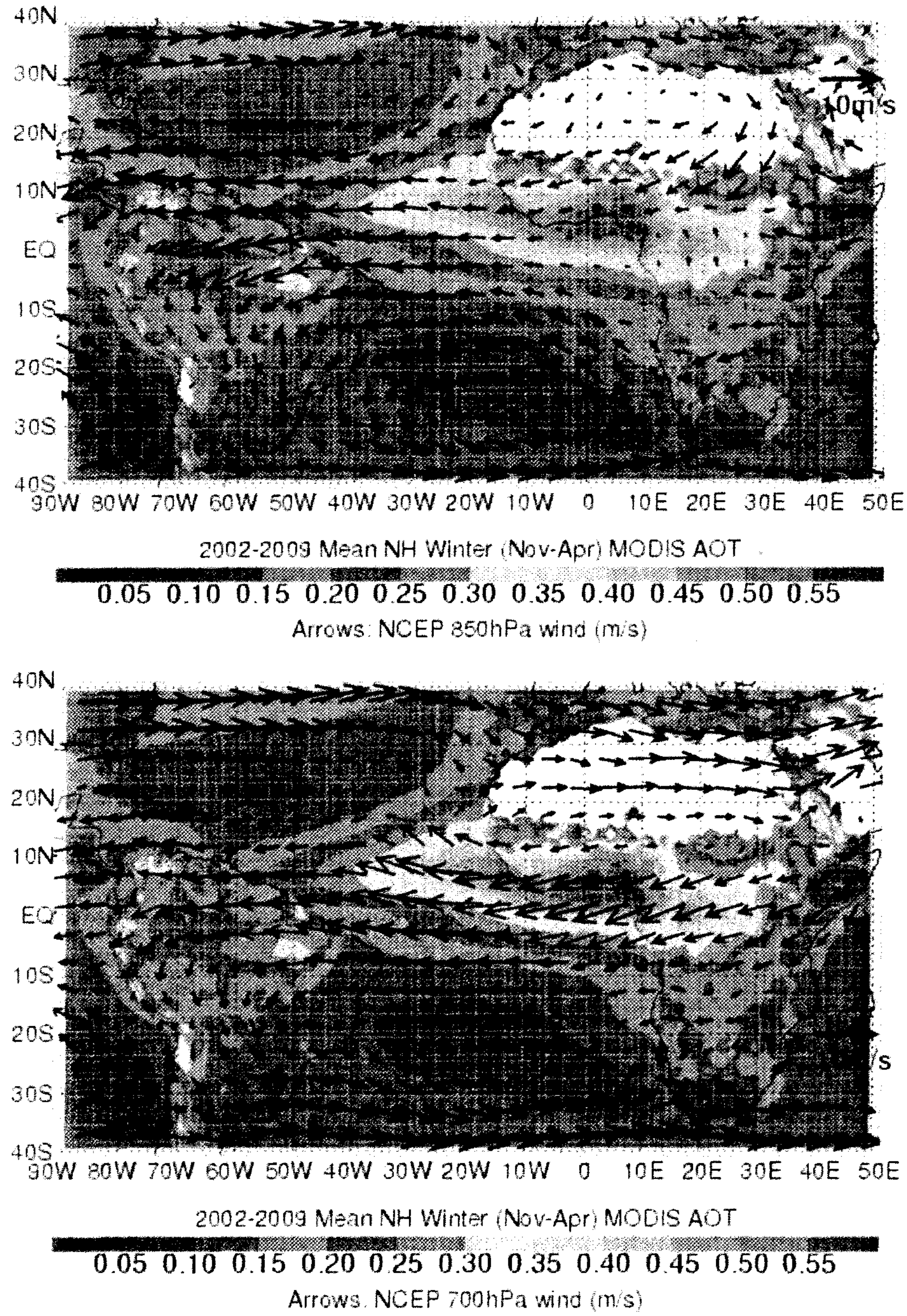

Figure 2: (a) Climatological mean (2002-2009) boreal winter (November-April) MODIS/Aqua AOT and NCEP/NCAR 850-hPa horizontal winds over the tropical Atlantic region. White regions indicate areas of missing MODIS/Aqua AOT data. (b) As in (a) except for 700-hPa NCEP/NCAR horizontal winds.

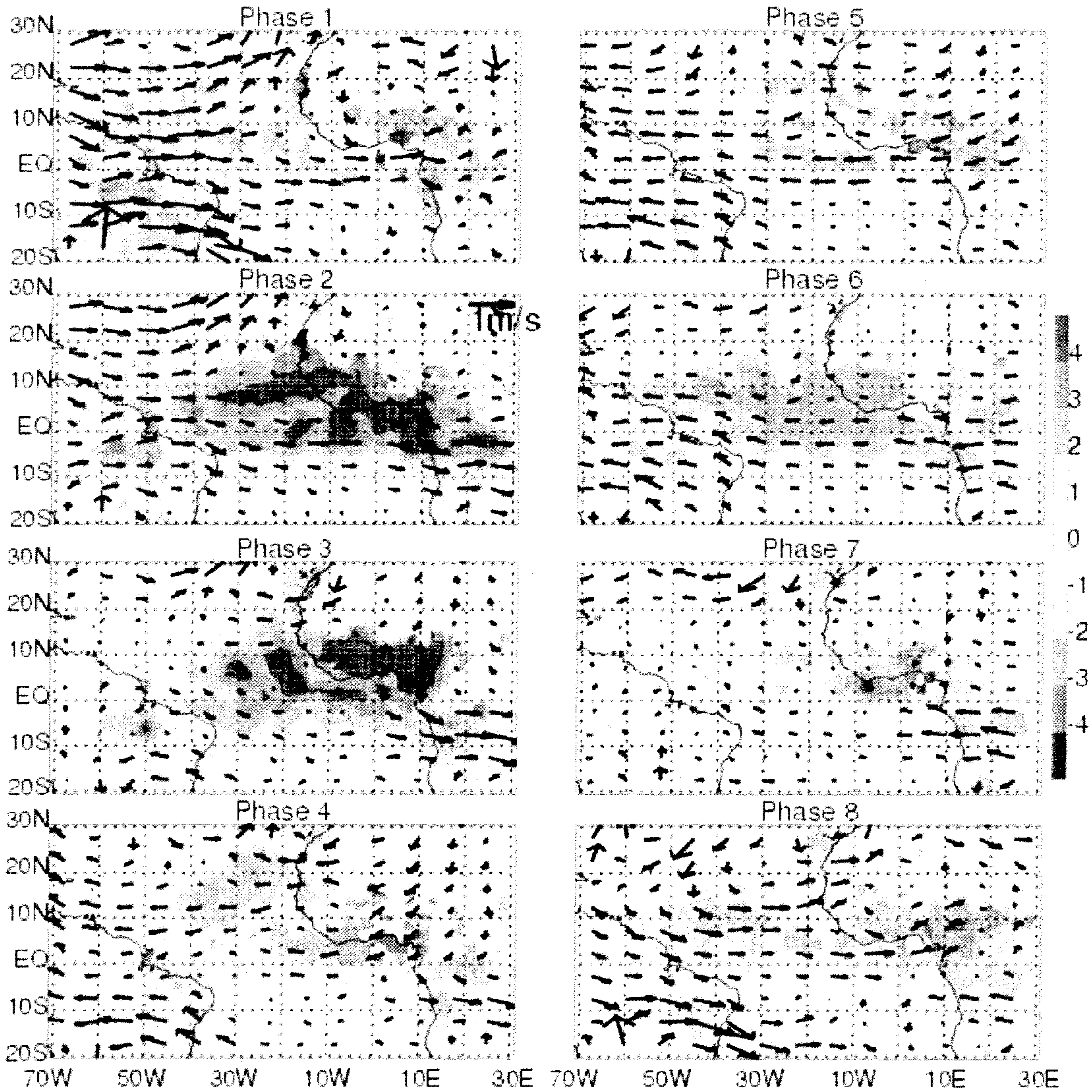

Figure 3: Composite maps of boreal winter (November-April) MJO-related MODIS/Aqua AOT anomalies (multiplied by 100) and NCEP/NCAR 850-hPa horizontal wind (m s^{-1}) anomalies over the tropical Atlantic region. Only AOT anomalies with above 95% confidence limit are shown.

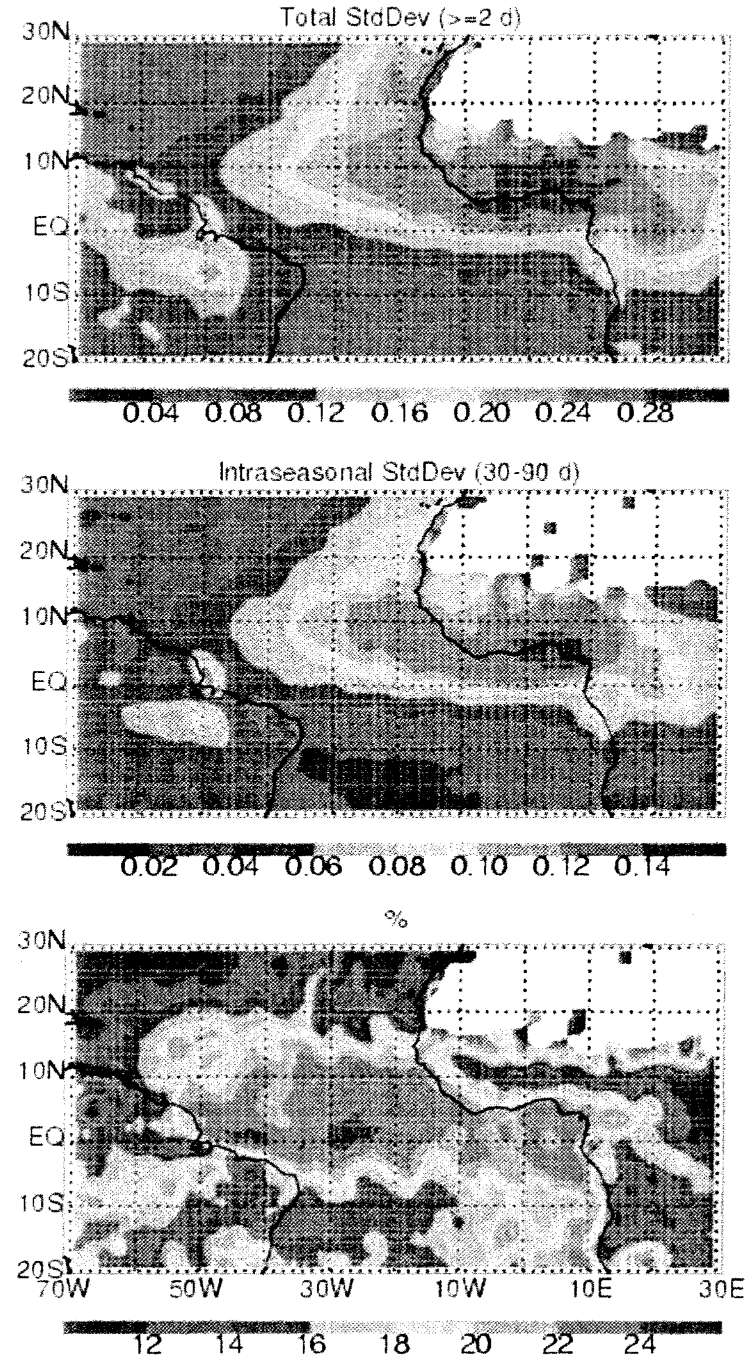

Figure 4: (a) Standard deviation of boreal winter (November-April) MODIS/Aqua AOT anomalies after removing the mean seasonal cycle (>= 2 days, total); (b) Same as (a) except for intraseasonal time scale after removing the mean seasonal cycle and filtering via a 30–90-day band pass filter; (c) Percentage of the total variance of boreal winter MOIDS/Aqua AOT anomalies explained by their intraseasonal variance.

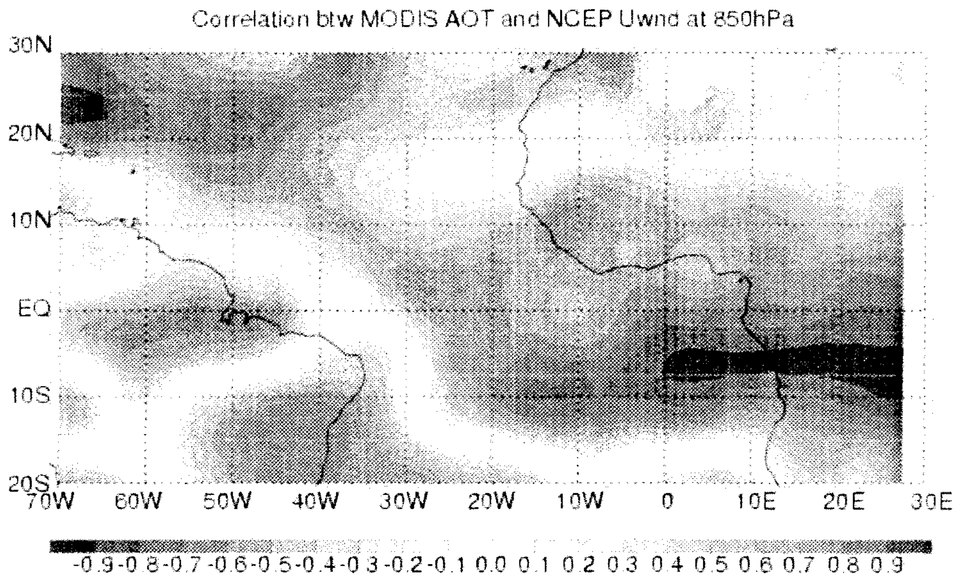

Figure 5: Linear correlation coefficient between boreal winter (November-April) MJO-related MODIS/Aqua AOT anomalies and NCEP/NCAR 850-hPa zonal wind (m s^{-1}) anomalies over the tropical Atlantic region. Negative (positive) correlation means that westerly anomalies induce negative (positive) AOT anomalies or easterly anomalies induce positive (negative) AOT anomalies.